PRAMANA — journal of physics

Vol. 57, No. 4
October 2001
pp. 743–754

Polarization modulational instability in a birefringent optical fiber with fourth order dispersion

R GANAPATHY and V C KURIAKOSE
Department of Physics, Cochin University of Science and Technology, Cochin 682 022, India
Email: ganapathyr@cusat.ac.in; vck@cusat.ac.in

MS received 9 October 2000; revised 30 March 2001

Abstract. We obtain conditions for the occurrence of polarization modulational instability in the anomalous and normal dispersion regimes for the coupled nonlinear Schrödinger equation modelling fourth order dispersion effects when the linearly polarized pump is oriented at arbitrary angles with respect to the slow and fast axes of the birefringent fiber.

Keywords. Birefringent optical fiber; fourth order dispersion; Floquet theory.

PACS Nos 42.81.Gs; 42.65.Sf; 42.65.Tg

1. Introduction

Modulational instability (MI) phenomenon in optical fibers manifests as breakup of continuous wave (cw) or quasi-cw radiation into a train of ultrashort pulses and happens when a cw perturbed radiation experiences an instability that leads to an exponential growth of its amplitude due to an interplay between fiber nonlinearity and group velocity dispersion [1]. Anomalous dispersion regime is a prerequisite for occurrence of MI in nonlinear Schrödinger equation (NLSE) which describes scalar beam propagation in optical fibers [1]. Beam propagation in an anisotropic medium such as a birefringent fiber is generally governed by coupled NLSE [1–3]. In a birefringent optical fiber, MI phenomena can be observed via two techniques; namely the single-frequency copropagation wherein two pump waves of identical frequency copropagate with orthogonal polarization parallel to the two birefringent axes of the fiber [4] and the two-frequency copropagation, where the two polarized waves copropagate with different frequencies [4]. Unlike in the case of NLSE, MI can occur in the normal dispersion regime for the coupled NLSE under certain specified conditions [5–7]. In polarization preserving birefringent optical fibers, MI may involve a change of the polarization state of an incident pump wave [8–10] as it traverses the fiber. This phenomenon is known as polarization MI (PMI) which is sensitive to the relative phase of the orthogonally polarized waves. Due to PMI, the incident pump wave which is polarized on one axis of the fiber, would generate orthogonally polarized Stokes and anti-Stokes sidebands. Trillo and Wabnitz, in their work, have analysed the role of nonlinear polarization of the pump on parametric amplification [11]. They have shown that PMI manifests as large changes in the output state of polarization when the input power or the polarization state is changed slightly. They attributed this phenomenon to the case when the linear beat length of the optical fiber becomes comparable to its nonlinear beat length for a specific input power.

MI phenomenon is useful for the generation for ultra short pulses which find applications in ultrafast all-optical switching devices capable of operating in high frequency regimes [12]. As the nonlinear polarization response of the birefringent optical fibers play a very crucial role in ultrashort pulse generation through pulse reshaping, a detailed analysis about PMI phenomenon is very much needed. MI phenomenon in presence of higher order dispersion effects results in ultrashort pulses with very high repetition rates which find applications in ultrafast all-optical switches [12]. In the present paper, considering the single-frequency copropagation regime, we study the influence of fourth order dispersion effects on PMI gain spectra of a linearly polarized intense pump wave which experiences periodic nonlinear polarization rotation in a birefringent optical fiber in both the anomalous and normal dispersion regimes.

The paper is arranged as follows: In §2, we briefly discuss the basic equation. In §3, using Floquet theorem we analyse the linear stability of a linearly polarized pump wave oriented at arbitrary angles with respect to the principal axes. In §4, we conclude.

2. Basic equation

An optically active medium such as a twisted birefringent optical fiber supports circularly polarized waves [11,14] and is represented by the following coupled higher order nonlinear Schrödinger equation (CHNSE):

$$
\begin{aligned}
i\,u_{\zeta} - G_1\,u_{\tau\tau} + 2\,p\,\left[|u|^2 + 2\,|v|^2\right]u - G_3\,u_{\tau\tau\tau\tau} + \frac{v}{2} &= 0,\\
i\,v_{\zeta} - G_1\,v_{\tau\tau} + 2\,p\,\left[|v|^2 + 2\,|u|^2\right]v - G_3\,v_{\tau\tau\tau\tau} + \frac{u}{2} &= 0,
\end{aligned}
\tag{1}
$$

where u and v are the normalized circular polarization components of the intensely polarized pump wave. ς is the dimensionless longitudinal distance and τ is the dimensionless retarded time. u_{ς} refers to partial derivative with respect to ς and so on. G_1 and G_3 denote group velocity dispersion and fourth order dispersion coefficients respectively. Since we are considering the single-frequency copropagation regime, G_1 and G_3 are considered to have the same value on both the slow and fast axes [4]. Equation (1) represents the continuous wave propagation in an optically active medium such as a twisted birefringent optical fiber which supports circularly polarized waves and which includes the effect due to fourth order dispersion. In this case, we have neglected the effects due to polarization walk off. We have also considered the case where the carrier frequency of continuous wave is at the extremum of the group velocity dispersion as a result of which the third order dispersion vanishes. We have further neglected other nonlinear effects such as stimulated Raman scattering (SRS), self-steepening, etc. as we are basically considering pulse propagation having pulse durations of the order of 500 femto seconds. At this range, the effect due to SRS can be neglected. Also at this range, the effects due to fourth order dispersion become high enough to influence the modulational instability (MI) phenomena. Cavalcanti *et al* have demonstrated experimentally the MI phenomena for the scalar nonlinear Schrödinger equation [13] where they have considered the effect due to fourth order dispersion with the second and fourth order dispersion coefficients at $-0.1\ \mathrm{ps}^2/\mathrm{Km}$ and $-7.0\ \mathrm{ps}^4/\mathrm{Km}$ respectively at the wavelength $\lambda = 1.32\ \mu$m. We have extended this to the case for a CHNSE. Moreover, we have considered a weakly birefringent fiber where the effects due to polarization walk-off can be neglected. The parameter p refers to normalized power.

3. Stability analysis and PMI phenomena

The state of polarization of a pump wave can be changed by introducing a phase shift between the two orthogonal polarization components of the pump wave [15]. Equation (1) admits steady state solutions of the form:

$$\begin{aligned} u(\varsigma) &= |U(\varsigma)|\ \exp\left(i\,\phi_1(\varsigma)\right), \\ v(\varsigma) &= |V(\varsigma)|\ \exp\left(i\,\phi_2(\varsigma)\right). \end{aligned} \tag{2}$$

On substituting eq. (2) in (1) we obtain the following expressions:

$$\begin{aligned} \frac{\mathrm{d}(|U|)}{\mathrm{d}\varsigma} &= \frac{|V|}{2}\ \sin\ \phi, \\ \frac{\mathrm{d}(|V|)}{\mathrm{d}\varsigma} &= -\frac{|U|}{2}\ \sin\ \phi, \\ \frac{\mathrm{d}(\phi_1)}{\mathrm{d}\varsigma} &= 2\,p\ \left(|U|^2 + 2\ |V|^2\right) + \frac{|V|}{2\ |U|}\ \cos\ \phi, \\ \frac{\mathrm{d}(\phi_2)}{\mathrm{d}\varsigma} &= 2\,p\ \left(2\,|U|^2 +\ |V|^2\right) + \frac{|U|}{2\ |V|}\ \cos\ \phi, \end{aligned} \tag{3}$$

where we have collected the real and imaginary terms of the above equation. The nonlinear phase shift $\phi = \phi_1 - \phi_2$ is responsible for the power dependent ellipse rotation of the pump wave. The local state of polarization of the pump is duly represented by the normalized Stokes parameters [11,14–16] which are of the form:

$$\begin{aligned} S_0(\varsigma) &= |U|^2 + |V|^2, \\ S_1(\varsigma) &= 2\ |U|\ |V|\ \cos\ \phi, \\ S_2(\varsigma) &= 2\ |U|\ |V|\ \sin\ \phi, \\ S_3(\varsigma) &= |V|^2 - |U|^2, \end{aligned} \tag{4}$$

such that $S_1^2(\varsigma) + S_2^2(\varsigma) + S_3^2(\varsigma) = 1$. On differentiating eq. (4) throughout with respect to ς and by using eq. (3), we obtain the equations to the Stokes parameters which are of the form:

$$\begin{aligned} \frac{\mathrm{d}S_1(\varsigma)}{\mathrm{d}\varsigma} &= -2\,p\,S_2(\varsigma)\ S_3(\varsigma), \\ \frac{\mathrm{d}S_2(\varsigma)}{\mathrm{d}\varsigma} &= S_3(\varsigma)\ \left(1 + 2\,p\ \ S_1(\varsigma)\right), \\ \frac{\mathrm{d}S_3(\varsigma)}{\mathrm{d}\varsigma} &= -S_2(\varsigma). \end{aligned} \tag{5}$$

From this set of equations, we obtain the expression $S_1(\varsigma) = S_{10} - p\, S_{30}^2 + p\, S_3^2(\varsigma)$ where S_{10} and S_{30} can be obtained from the initial conditions. From eq. (5) we obtain an equation of the form

$$\left(\frac{\mathrm{d}S_3(\varsigma)}{\mathrm{d}\varsigma}\right)^2 = p^2\,\left(\alpha_1 - S_3^2(\varsigma)\right)\,\left(\alpha_2 + S_3^2(\varsigma)\right), \tag{6}$$

where

$$\alpha_1 = \frac{1}{2\,p^2}\,\left(-\left(1 + 2\,p\,S_{10}\right) + \sqrt{\left(1 + 2\,p\,S_{10}\right)^2 + 4\,p^2\,S_{20}^2}\right)$$

and

$$\alpha_2 = \frac{1}{2\,p^2}\,\left(\left(1 + 2\,p\,S_{10}\right) + \sqrt{\left(1 + 2\,p\,S_{10}\right)^2 + 4\,p^2\,S_{20}^2}\right).$$

S_{20} can also be obtained from the initial conditions. Equation (6) can be solved using Jacobian elliptical functions of the first kind to obtain:

$$S_3(\varsigma) = -\frac{S_{20}}{f}\, sd\,(f\,\varsigma;\, m), \tag{7}$$

where $f = \left(1 + 4\,p^2 + 4\,p\,S_{10}\right)^{0.25}$ and the Jacobian parameter, $m = 0.5\,\left(1 - \frac{1+2\,p\,S_{10}}{f^2}\right)$. Therefore,

$$S_2(\varsigma) = -\frac{\mathrm{d}\,S_3(\varsigma)}{\mathrm{d}\,\varsigma} = S_{20}\, cd\,(f\,\varsigma;\, m)\; nd\,(f\,\varsigma;\, m) \tag{8}$$

and

$$S_1(\varsigma) = S_{10} - p\,S_{30}^2 + p\,S_3^2(\varsigma). \tag{9}$$

sd, *nd* and *cd* are the Jacobian elliptic functions of first kind [17]. Thus eqs (7), (8) and (9) represent the pump wave evolution. For a linearly polarized pump wave,

$$\begin{aligned} S_{10} &= \cos(2\theta), \\ S_{20} &= \sin(2\theta), \\ S_{30} &= 0, \end{aligned} \tag{10}$$

where θ is the angle of orientation of the pump wave with respect to the slow axis.

So far we have considered the steady state solution. Now we consider a perturbation procedure where we slightly perturb the steady state solutions first by considering only the spatial evolution (ie. at $\tau = 0$) of the perturbing amplitudes and then including the temporal evolution of the perturbing amplitudes as well which are in the form of Stokes and anti-Stokes side-band amplitudes [11]. We also consider the approximation that higher harmonics do not significantly influence the system dynamics. Now, at $\tau = 0$, the amplitudes of the two polarization components are perturbed slightly to obtain:

$$\begin{aligned} u(\varsigma) &= \left(|U(\varsigma)| + u_0'(\varsigma)\right)\, \exp\left(i\,\phi_1(\varsigma)\right), \\ v(\varsigma) &= \left(|V(\varsigma)| + v_0'(\varsigma)\right)\, \exp\left(i\,\phi_2(\varsigma)\right). \end{aligned} \tag{11}$$

On substituting eq. (11) into eq. (1), the coupled equations to the spatial dependance of the perturbed pump fields are of the form:

$$
\begin{aligned}
-i\,\frac{\partial u_0'(\varsigma)}{\partial \varsigma} = {} & \left(p\,\left(1-S_3(\varsigma)\right) - \frac{S_1(\varsigma)}{2\,\left(1-S_3(\varsigma)\right)}\right) u_0'(\varsigma) \\
& + p\,\left(1-S_3(\varsigma)\right)\, u_0'^{*}(\varsigma) \\
& + \left(0.5\,\frac{\left(S_1(\varsigma)-i\,S_2(\varsigma)\right)}{\sqrt{1-S_3^2(\varsigma)}} + 2\,p\,\sqrt{1-S_3^2(\varsigma)}\right) v_0'(\varsigma) \\
& + 2\,p\,\sqrt{1-S_3^2(\varsigma)}\, v_0'^{*}(\varsigma), \\
-i\,\frac{\partial v_0'(\varsigma)}{\partial \varsigma} = {} & \left(0.5\,\frac{\left(S_1(\varsigma)+i\,S_2(\varsigma)\right)}{\sqrt{1-S_3^2(\varsigma)}} + 2\,p\,\sqrt{1-S_3^2(\varsigma)}\right) u_0'(\varsigma) \\
& + 2\,p\,\sqrt{1-S_3^2(\varsigma)}\, u_0'^{*}(\varsigma) \\
& + \left(p\,\left(1+S_3(\varsigma)\right) - \frac{S_1(\varsigma)}{2\,\left(1+S_3(\varsigma)\right)}\right) v_0'(\varsigma) \\
& + p\,\left(1+S_3(\varsigma)\right)\, v_0'^{*}(\varsigma),
\end{aligned}
\qquad (12)
$$

where u_0' and v_0' denote the spatial evolution of the perturbing amplitudes at $\tau = 0$. In order to study the temporal evolution of the perturbing amplitudes as well, we next consider the full fledged spatio-temporal evolution of the perturbing amplitudes $u_0(\varsigma,\tau)$ and $v_0(\varsigma,\tau)$ which are given by

$$
\begin{aligned}
u_0(\varsigma,\tau) &= u_{10}(\varsigma)\,\exp(i\,\Omega\,\tau) + u_{20}(\varsigma)\,\exp(-i\,\Omega\,\tau), \\
v_0(\varsigma,\tau) &= v_{10}(\varsigma)\,\exp(i\,\Omega\,\tau) + v_{20}(\varsigma)\,\exp(-i\,\Omega\,\tau),
\end{aligned}
\qquad (13)
$$

where $\left(u_{10}, v_{10}\right)$ and $\left(u_{20}, v_{20}\right)$ are the amplitudes of Stokes and anti-Stokes side bands respectively. Throughout, we have assumed that $\left|u_0\right| \ll |U|$ and $\left|v_0\right| \ll |V|$. The perturbed equations are given by

$$
\begin{aligned}
u(\varsigma,\tau) &= \left(|U(\varsigma)| + u_0(\varsigma,\tau)\right)\,\exp\left(i\,\phi_1(\varsigma)\right), \\
v(\varsigma,\tau) &= \left(|V(\varsigma)| + v_0(\varsigma,\tau)\right)\,\exp\left(i\,\phi_2(\varsigma)\right).
\end{aligned}
\qquad (14)
$$

Now we replace u_0' and v_0' with $u_0(\varsigma,\tau)$ and $v_0(\varsigma,\tau)$ in eq. (12) and substituting this along with eqs (13) and (14) into eq. (1) and on linearizing with respect to u_{10}, u_{20}^*, v_{10} and v_{20}^*, we finally arrive at the following set of coupled linear differential equations in terms of the perturbing fields $u_{10}(\varsigma)$, $u_{20}^*(\varsigma)$, $v_{10}(\varsigma)$ and $v_{20}^*(\varsigma)$ which are of the form:

$$
\begin{aligned}
-i\,\frac{\mathrm{d}u_{10}(\varsigma)}{\mathrm{d}\varsigma} = {} & m_{11}(\varsigma)\,u_{10}(\varsigma) + m_{12}(\varsigma)\,u_{20}^*(\varsigma) \\
& + m_{13}(\varsigma)\,v_{10}(\varsigma) + m_{14}(\varsigma)\,v_{20}^*(\varsigma), \\
-i\,\frac{\mathrm{d}u_{20}^*(\varsigma)}{\mathrm{d}\varsigma} = {} & m_{21}(\varsigma)\,u_{10}(\varsigma) + m_{22}(\varsigma)\,u_{20}^*(\varsigma)
\end{aligned}
$$

$$
\begin{aligned}
&\qquad + m_{23}(\varsigma)\ v_{10}(\varsigma) + m_{24}(\varsigma)\ v_{20}^{*}(\varsigma),\\
-i\,\frac{\mathrm{d}v_{10}(\varsigma)}{\mathrm{d}\varsigma} &= m_{31}(\varsigma)\ u_{10}(\varsigma) + m_{32}(\varsigma)\ u_{20}^{*}(\varsigma)\\
&\qquad + m_{33}(\varsigma)\ v_{10}(\varsigma) + m_{34}(\varsigma)\ v_{20}^{*}(\varsigma),\\
-i\,\frac{\mathrm{d}v_{20}^{*}(\varsigma)}{\mathrm{d}\varsigma} &= m_{41}(\varsigma)\ u_{10}(\varsigma) + m_{42}(\varsigma)\ u_{20}^{*}(\varsigma)\\
&\qquad + m_{43}(\varsigma)\ v_{10}(\varsigma) + m_{44}(\varsigma)\ v_{20}^{*}(\varsigma),
\end{aligned}
\tag{15}
$$

where

$$
\begin{aligned}
m_{11}(\varsigma) &= G_1\,\Omega^2 - G_3\,\Omega^4 + p\ \left(1 - S_3(\varsigma)\right) - \frac{S_1(\varsigma)}{2\left(1 - S_3(\varsigma)\right)},\\
m_{12}(\varsigma) &= p\ \left(1 - S_3(\varsigma)\right),\\
m_{13}(\varsigma) &= \frac{0.5\ \left(S_1(\varsigma) - i\,S_2(\varsigma)\right)}{\sqrt{1 - \left(S_3(\varsigma)\right)^2}} + 2\,p\,\sqrt{1 - \left(S_3(\varsigma)\right)^2},\\
m_{14}(\varsigma) &= 2\,p\,\sqrt{1 - \left(S_3(\varsigma)\right)^2},
\end{aligned}
\tag{16}
$$

$$
\begin{aligned}
m_{21}(\varsigma) &= -p\ \left(1 - S_3(\varsigma)\right),\\
m_{22}(\varsigma) &= -\left(G_1\,\Omega^2 - G_3\,\Omega^4 + p\ \left(1 - S_3(\varsigma)\right) - \frac{S_1(\varsigma)}{2\left(1 - S_3(\varsigma)\right)}\right),\\
m_{23}(\varsigma) &= -2\,p\,\sqrt{1 - \left(S_3(\varsigma)\right)^2},\\
m_{24}(\varsigma) &= -\left(0.5\ \frac{\left(S_1(\varsigma) + i\,S_2(\varsigma)\right)}{\sqrt{1 - \left(S_3(\varsigma)\right)^2}} + 2\,p\,\sqrt{1 - \left(S_3(\varsigma)\right)^2}\right),
\end{aligned}
\tag{17}
$$

$$
\begin{aligned}
m_{31}(\varsigma) &= \frac{0.5\ \left(S_1(\varsigma) + i\,S_2(\varsigma)\right)}{\sqrt{1 - \left(S_3(\varsigma)\right)^2}} + 2\,p\,\sqrt{1 - \left(S_3(\varsigma)\right)^2},\\
m_{32}(\varsigma) &= 2\,p\,\sqrt{1 - \left(S_3(\varsigma)\right)^2},\\
m_{33}(\varsigma) &= G_1\,\Omega^2 - G_3\,\Omega^4 + p\ \left(1 + S_3(\varsigma)\right) - \frac{S_1(\varsigma)}{2\left(1 + S_3(\varsigma)\right)},\\
m_{34}(\varsigma) &= p\ \left(1 + S_3(\varsigma)\right),
\end{aligned}
\tag{18}
$$

and

$$
\begin{aligned}
m_{41}(\varsigma) &= -2\,p\,\sqrt{1 - \left(S_3(\varsigma)\right)^2},\\
m_{42}(\varsigma) &= -\left(0.5\ \frac{\left(S_1(\varsigma) - i\,S_2(\varsigma)\right)}{\sqrt{1 - \left(S_3(\varsigma)\right)^2}} + 2\,p\,\sqrt{1 - \left(S_3(\varsigma)\right)^2}\right),
\end{aligned}
$$

$$m_{43}(\varsigma) = -p\,\left(1+S_3(\varsigma)\right),$$
$$m_{44}(\varsigma) = -\left(G_1\,\Omega^2 - G_3\,\Omega^4 + p\,\left(1+S_3(\varsigma)\right) - \frac{S_1(\varsigma)}{2\left(1+S_3(\varsigma)\right)}\right). \tag{19}$$

Equation (15) can be represented in the matrix form as

$$\frac{\mathrm{d}\mathbf{X}(\varsigma)}{\mathrm{d}\varsigma} = \mathbf{M}(\varsigma)\;\mathbf{X}(\varsigma), \tag{20}$$

where $\mathbf{X}(\varsigma) = \left(u_{10}, u_{20}^*, v_{10}, v_{20}^*\right)^T$ and the superscript T denotes transpose. $\mathbf{M}(\varsigma)$is a complex periodic matrix with period given by $\varsigma_p = 4\,K(m)/f$, where $K(m)$ is a complete elliptic integral of the first kind. ς_p is defined as the normalized nonlinear beat length of the optical fiber.

Equation (20) is a linear homogenous (LH) system with periodic coefficients. The LH system is solved using Floquet theorem [19] as follows: The periodic matrix $\mathbf{M}(\varsigma)$ has distinct eigenvalues for all values of ς and frequency detuning parameter Ω. Hence the corresponding eigenvectors would be linearly independent. Let $\mathbf{P}(\varsigma)$ denote a periodic matrix with the linearly independent eigenvectors written side by side. Then the solution to eq. (20) is given by Floquet theorem as

$$\Phi(\varsigma) = \;\mathbf{P}(\varsigma)\;\exp(\mathbf{B}\,\varsigma), \tag{21}$$

where the nonsingular matrix $\mathbf{B}$ is written as

$$\mathbf{B} = \mathbf{P}^{-1}(\varsigma=\varsigma_p)\;\mathbf{M}(\varsigma=\varsigma_p)\;\mathbf{P}(\varsigma=\varsigma_p) - \;\mathbf{P}^{-1}(\varsigma=\varsigma_p)\;\left(\frac{\mathrm{d}\mathbf{P}(\varsigma)}{\mathrm{d}\varsigma}\right)_{\varsigma=\varsigma_p}. \tag{22}$$

$\Phi(\varsigma)$ is known as the fundamental matrix with the property that

$$\Phi(\varsigma+\varsigma_p) = \Phi(\varsigma)\;\exp(\mathbf{B}\,\varsigma_p). \tag{23}$$

The normalized form of eq. (21) is known as the state transition matrix $\mathbf{L}(\varsigma)$ which is given by

$$\mathbf{L}(\varsigma) = \Phi(\varsigma)\;\Phi^{-1}(\varsigma=0). \tag{24}$$

Therefore

$$\mathbf{L}(\varsigma=\varsigma_p) = \exp(\mathbf{B}\,\varsigma_p). \tag{25}$$

In order to obtain $\mathbf{L}(\varsigma=\varsigma_p)$ numerically, we choose $\mathbf{L}(\varsigma=0)$ to be the unit matrix of order 4, such that each column vector of $\mathbf{L}(\varsigma=0)$ depicts linearly independent initial conditions for eq. (20). With this set of initial conditions, we numerically solve eq. (20) using the Runge–Kutta–Gill method [18] in order to obtain $\mathbf{L}(\varsigma=\varsigma_p)$. As the next procedure, the eigenvalues Λ of $\mathbf{L}(\varsigma=\varsigma_p)$ known as Floquet multilpiers are determined which are distinct. The instability condition is satisfied only if $|\Lambda| > 1$ [11]. The eigenvalues σ of the nonsingular matrix $\mathbf{B}$ are known as Floquet exponents. Floquet theorem connects

σ and Λ via the relation $\Lambda = \exp(\sigma\, \varsigma_p)$ [19] which is clear from eq. (25). Thus the unstable side-band power gain G is given by the relation $G = 2/\varsigma_p \ln|\Lambda|$ [11]. Using the above relation, one can draw parametric gain curves as functions of finite frequency detuning Ω as is clear from the linear homogeneous system given by eq. (20) and thereby eq. (25) for both the anomalous and normal dispersion regimes. Figures 1a and 1b show the growth rate curves as functions of Ω when the linearly polarized pump wave is oriented at $\theta = 1^\circ$ from the slow axis of the birefringent fiber for various values of the normalized power coefficient p and for the fourth order dispersion coefficient $G_3 = 0.005$ drawn for anomalous and normal dispersion regimes respectively. The variation of the unstable parametric gain for various values of p when the linearly polarized pump wave is oriented at $\theta = 1^\circ$ from the fast axis for the case of anomalous and normal dispersion regimes are shown in figures 2 and 3 respectively. It is observed that the parametric gain curve virtually remains the same whenever the pump is rotated from the slow axis by a few degrees for both the regimes. Also, when the linearly polarized pump wave is oriented close to the fast axis, below $p = 0.5$ no MI is observed. As the value of p is steadily increased thereafter, the parametric gain curve is found to vary considerably for various values of p thereby confirming the fact that the slow and the fast axes of a polarization preserving fiber are not equivalent when one considers the influence of the fourth order dispersion effects also. Figures 4, 5 and 6 depict this property of the parametric gain curve for various values of p when the linearly polarized pump wave is oriented at 1° from the fast axis for the normal and anomalous dispersion regimes respectively. In order to obtain the final form of $u(\varsigma,\tau)$ and $v(\varsigma,\tau)$, we plot numerically eq. (14) at $\varsigma = \varsigma_p$ for various values of τ and finite frequency detuning Ω under the approximation that higher harmonics do not significantly influence the system dynamics. Figures 7 and 8 show the plots of

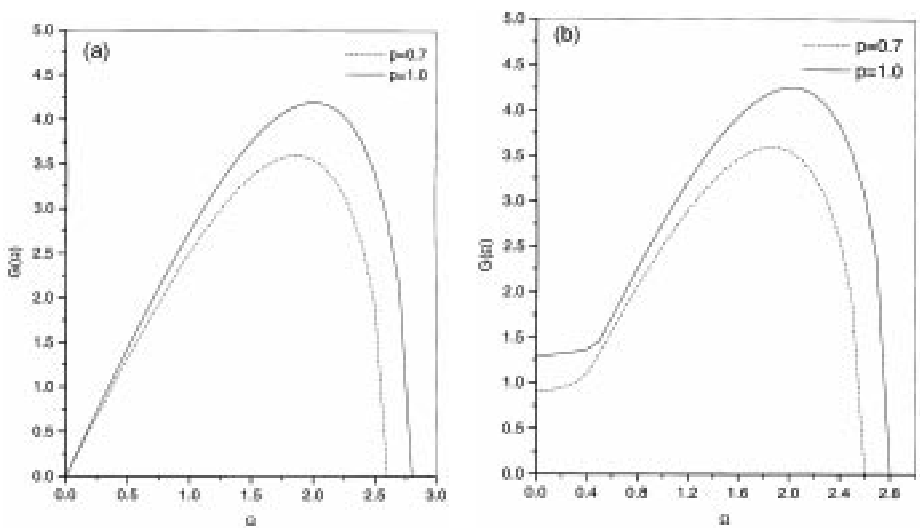

Figure 1. Graphical relation between the parametric gain curve and the frequency detuning for $p = 1.0$ and 0.7 and $G_3 = 0.005$ when the pump is oriented at an angle of 1° from the slow axis for (**a**) the anomalous dispersion regime and (**b**) the normal dispersion regime.

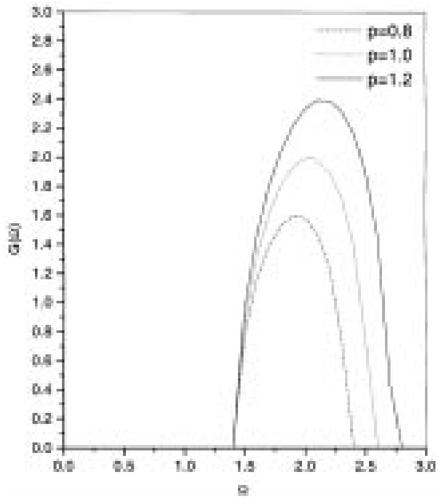

Figure 2. Graphical relation between the parametric gain curve and the frequency detuning for $p = 1.2,\ 1.0$ and 0.8 and $G_3 = 0.005$ when the pump is oriented at an angle of 1° from the fast axis for the anomalous dispersion regime.

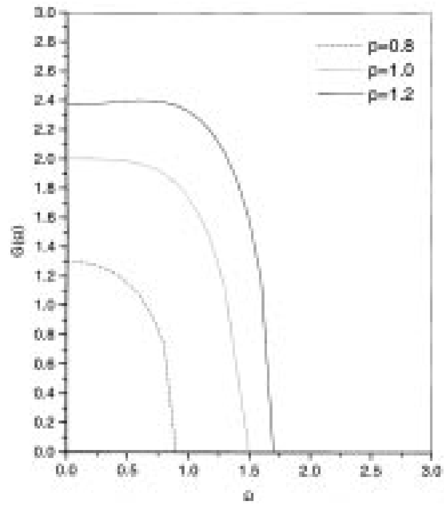

Figure 3. Graphical relation between the parametric gain curve and the frequency detuning for $p = 1.2,\ 1.0$ and 0.8 and $G_3 = 0.005$ when the pump is oriented at an angle of 1° from the fast axis for the normal dispersion regime.

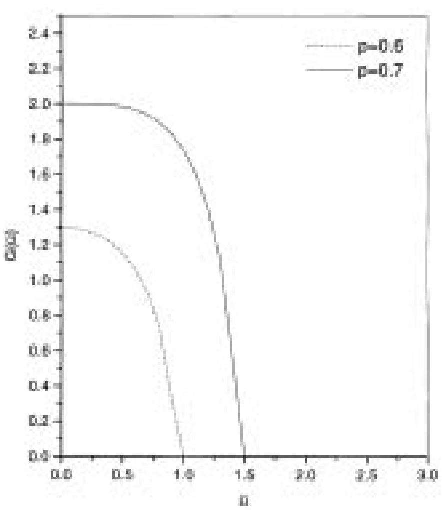

Figure 4. Graphical relation between the parametric gain curve and the frequency detuning for $p = 0.7$ and 0.6 and $G_3 = 0.005$ when the pump is oriented at an angle of 1° from the fast axis for the normal dispersion regime.

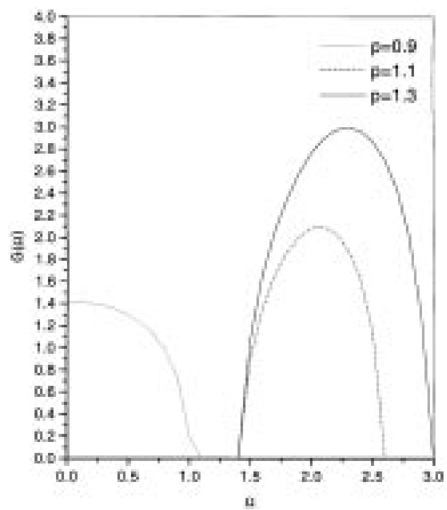

Figure 5. Graphical relation between the parametric gain curve and the frequency detuning for $p = 1.3,\ 1.1$ and 0.9 and $G_3 = 0.005$ when the pump is oriented at an angle of 1° from the fast axis for the normal dispersion regime.

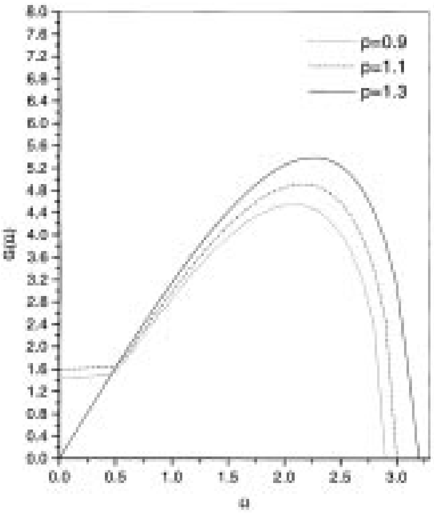

Figure 6. Graphical relation between the parametric gain curve and the frequency detuning for $p = 1.3,\ 1.1$ and 0.9 and $G_3 = 0.005$ when the pump is oriented at an angle of 1° from the fast axis for the anomalous dispersion regime.

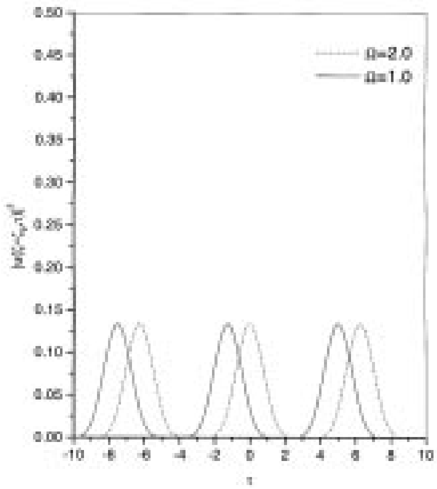

Figure 7. Plots of $\left|u\left(\varsigma = \varsigma_p, \tau\right)\right|^2$ versus τ for various values of Ω in the anomalous dispersion regime when the linearly polarized pump wave is oriented at an angle of 1° from the slow axis.

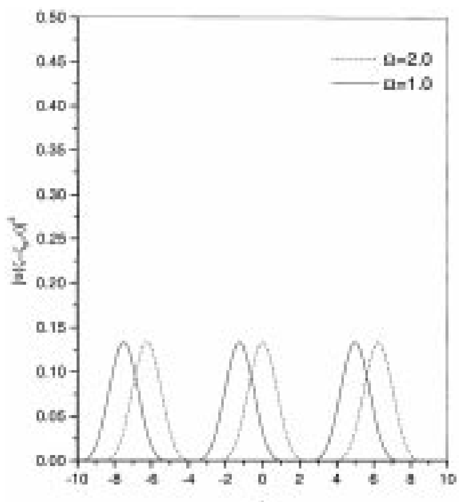

Figure 8. Plots of $|u(\varsigma = \varsigma_p, \tau)|^2$ versus τ for various values of Ω in the normal dispersion regime when the linearly polarized pump wave is oriented at an angle of 1° from the slow axis.

$\left|u\left(\varsigma = \varsigma_p, \tau\right)\right|^2$ versus τ for various values of Ω in the anomalous and normal dispersion regimes respectively. Similar plots can be obtained for $\left|v\left(\varsigma = \varsigma_p, \tau\right)\right|^2$. We are able to retrieve the results of ref. [12] for $G_3 = 0.0$. Thus we can arrive at the conclusion that even for a polarization preserving fiber, large asymmetry exists between the slow and the fast axes for continuous wave evolutions in the case of both the anomalous and normal dispersion regimes. In order to obtain the exact nature of the solutions for the case when the pump wave is oriented at arbitrary angles with respect to the axes, one has to employ direct numerical simulation of eq. (1). A study of this type of work is in progress.

4. Conclusions

Using Floquet theory, the unstable power gain is obtained as function of fine frequency side-band detuning when a linearly polarized pump wave is oriented at arbitrary angles with respect to the slow and fast axes for the anomalous and normal dispersion regimes on considering fourth order dispersion effects. It is observed that the parametric gain curve virtually remains the same whenever the pump is rotated from the slow axis by a few degrees for both the regimes. Also, when the linearly polarized pump wave is oriented close to the fast axis, below $p = 0.5$ no MI is observed. As the value of p is steadily increased thereafter, the parametric gain curve is found to vary considerably for various values of p thereby confirming the fact that the slow and the fast axes of a polarization preserving fiber are not equivalent when one considers the influence of the fourth order dispersion effects also.

Acknowledgements

The authors are thankful to the referee for valuable comments. VCK acknowledges Associateship of IUCAA, Pune.

References

[1] G P Agrawal, *Nonlinear fiber optics* (Academic Press, New York, 1995)
[2] N N Akhmediev and A V Buryak, *Opt. Comm.* **121**, 109 (1995)
[3] C R Menyuk, *IEEE J. Quant. Electron.* **25**, 2674 (1989)
[4] E Steve, P Tchofo Dinda, G Millot and M Remoissent, *Phys. Rev.* **A54**, 3519 (1996)
[5] G P Agrawal, *Phys. Rev. Lett.* **59**, 880 (1987)
[6] S Wabnitz, *Phys. Rev.* **A38**, 2018 (1988)
[7] J E Rothenberg, *Phys. Rev.* **A42**, 682 (1990)
[8] S Trillo and S Wabnitz, *J. Opt. Soc. Am.* **B6**, 238 (1989)
[9] S G Murdoch, R Leonhardt and J D Harvey, *Opt. Lett.* **20**, 866 (1995)
[10] G Gregori and S Wabnitz, *Phys. Rev. Lett.* **56**, 600 (1986)
[11] S Trillo and S Wabnitz, *Phys. Rev.* **E56**, 1048 (1997)
[12] M N Islam, S P Dijaili and J P Gordon, *Opt. Lett.* **13**, 518 (1988)
[13] S B Cavalcanti, J C Cressoni, H R da Cruz and A S Gouveia-Neto, *Phys. Rev.* **A43**, 6162 (1991)
[14] A Hasegawa and Y Kodama, *Solitons in optical communications* (Clarendon Press, Oxford, 1995)
[15] E Collett, *Polarized light – fundamentals and applications* (Marker Dekker Inc., 1993)

[16] K Sala, *Phys. Rev.* **A29**, 1944 (1984)
[17] P F Byrd and M D Friedman, *Handbook of elliptic integrals for engineers and scientists* (Springer-Verlag, New York, 1971)
[18] H M Antia, *Numerical methods for scientists and engineers* (Tata McGraw-Hill, New Delhi, 1991)
[19] E A Coddington and N Levison, *Theory of ordinary differential equations* (McGraw-Hill, New York, 1955)